Experimental Cell Research 382 (2019) 111486

Contents lists available at ScienceDirect

Experimental Cell Research

journal homepage: www.elsevier.com/locate/yexcr

# NETs promote ALI/ARDS inflammation by regulating alveolar macrophage polarization

Chao Song[a], Haitao Li[a], Yi Li[a], Minhui Dai[a], Lemeng Zhang[b], Shuai Liu[a], Hongyi Tan[c], Pengbo Deng[a], Jingjing Liu[a], Zhi Mao[a], Qian Li[a], Xiaoli Su[a], Yuan Long[a], Fengyu Lin[a], Yanjun Zeng[a], Yifei Fan[a], Bailing Luo[a], Chengping Hu[a], Pinhua Pan[a,*]

[a] Respiratory Department, Xiangya Hospital, Central South University, China
[b] Cancer Hospital of Hunan Province, China
[c] Central Hospital, Changsha, Hunan Province, China

ARTICLE INFO

*Keywords:*
M1-like macrophage polarization
NET inhibitor
Neutrophil
BMDM

ABSTRACT

Neutrophils activated during acute lung injury (ALI) form neutrophil extracellular traps (NETs) to capture pathogens. However, excessive NETs can cause severe inflammatory reactions. Macrophages are classified as M1 macrophages with proinflammatory effects or M2 macrophages with anti-inflammatory effects. During ALI, alveolar macrophages (AMs) polarize to the M1 phenotype. This study tested the hypothesis that NETs may aggravate ALI or acute respiratory distress syndrome (ARDS) inflammation by promoting alveolar macrophage polarization to the M1 type. Our research was carried out in three aspects: clinical research, animal experiments and in vitro experiments. We determined that NET levels in ARDS patients were positively correlated with M1-like macrophage polarization. NET formation was detected in murine ALI tissue and associated with increased M1 markers and decreased M2 markers in BALF and lung tissue. Treatment with NET inhibitors significantly inhibitor NETs generation, downregulated M1 markers and upregulated M2 markers. Regardless of LPS prestimulation, significant secretion of proinflammatory cytokines and upregulated M1 markers were detected from bone marrow-derived macrophages (M0 and M2) cocultured with high concentrations of NETs; conversely, M2 markers were downregulated. In conclusion, NETs promote ARDS inflammation during the acute phase by promoting macrophage polarization to the M1 phenotype. We propose that NETs play an important role in the interaction between neutrophils and macrophages during the early acute phase of ALI.

## 1. Introduction

Acute respiratory distress syndrome (ARDS) is a clinical syndrome characterized by a wide range of inflammatory reactions in the lungs, usually secondary to pneumonia, sepsis, and trauma (infection is the primary cause of ARDS) [1]. During acute lung inflammation, neutrophils and alveolar macrophages (AMs) account for more than 90% of the total bronchoalveolar lavage fluid (BALF) cells and are the main inflammatory cells during the development of ALI/ARDS [2].

AMs are the predominant leukocyte phenotype in the lung among all age groups (> 89%). AMs are usually in the resting state (M0). Activated AMs can be divided into two main phenotypes: M1 and M2 macrophages [3]. M1 macrophages encourage inflammation by secreting proinflammatory cytokines, such as IL-1 β, IL-12, TNF-α, IL-6, and inducible nitric oxide synthase (iNOS). M2 macrophages contribute to tissue repair due to their anti-inflammatory functions, which are mediated by the release of Th2 cytokines, such as IL-4, IL-10, and IL-13 [4,5]. Circulating monocytes and macrophages are recruited to the alveolar space and activated by macrophage colony-stimulating factor (M-CSF) mediators produced by T cells, macrophages, endothelial cells, and fibroblasts. M1 macrophages release toxic species, such as nitric oxide, superoxide, and matrix metalloproteinases, which cause tissue damage. The TNF-α and IL-1β produced by macrophages also activate neutrophils and induce the overexpression of adhesion molecules, such as intercellular adhesion molecule 1 and vascular cell adhesion molecule 1, on immune cells and endothelial cells [6–8]. High concentrations of TNF-α and IL-1β have been reported in BALF from ARDS patients [9,10]. During the early inflammatory phage of ARDS, resident alveolar macrophages are activated [11], leading to the release of potent proinflammatory mediators and chemokines that promote the accumulation of neutrophils and monocytes, and the proportion of M1/M2 macrophages becomes unbalanced, leading to increased

* Corresponding author. Respiratory Department, Xiangya Hospital, Central South University, 87 Xiangya roud, Changsha, Hunan Province, China.
*E-mail address:* pinhuapan668@csu.edu.cn (P. Pan).

https://doi.org/10.1016/j.yexcr.2019.06.031
Received 19 March 2019; Received in revised form 23 June 2019; Accepted 24 June 2019
Available online 28 June 2019

inflammation and further tissue damage, which was confirmed in our experiment (the results of this part are not shown in the article; see S1 for details.). In vitro, M1 polarization can be stimulated by LPS/IFN-γ, and M2 polarization is related to IL-4 or IL-13 [12,13].

Neutrophils are thought to be the primary innate immune cells that cause damage to host tissues. In addition to exhibiting phagocytic activity against pathogenic bacteria and releasing antimicrobial molecules, neutrophils also form neutrophil extracellular traps (NETs) to regulate the severity of infection. NETs consist of deagglomerated chromatin fibers coated with antimicrobial proteins, such as histones, neutrophil elastase (NE), myeloperoxidase (MPO) and alpha-defensins. In addition to being expressed on NET fibers, NE and MPO also regulate NET formation [8,14,15]. NETs can effectively capture and kill pathogens. However, there is increasing evidence that overproduction of NETs can lead to severe inflammatory reactions and tissue damage [16,17].

Cathelicidin LL-37 is a cationic peptide that is synthesized by neutrophils, monocytes, keratinocytes and macrophages and is one of the antimicrobial peptides of NETs. LL-37 can stimulate immunocyte chemotaxis, promote M1 macrophage differentiation [18]. Macrophage can phagocytose non-apoptotic and apoptotic neutrophils, as well as MPO in neutrophils (especially via macrophage mannose receptors) [19]. Ingestion of apoptotic neutrophils can cause macrophage M2 repair-like phenotypes, whereas ingestion of MPO results in increased inflammatory cytokine release, similar to the M1-like macrophage phenotype [19].

Our previous experimental results showed that in the LPS ALI/ARDS mouse model, NETs are significantly increased, and the use of DNase (DNase I) can degrade NETs and suppress the inflammatory response [20]. In this article, we hypothesized that NETs may aggravate tissue injury in the exudative phase of ARDS by promoting the polarization of alveolar macrophages to the M1 subtype.

## 2. Materials and methods

### 2.1. Clinical research

#### 2.1.1. Research subjects

According to the Berlin definition of ARDS [1], a group of 20 patients (Table 1 lists the basic information of the patients. See S5 for details) with ARDS were studied in a respiratory intensive care unit (ICU) and central ICU in Xiangya Hospital. We collected samples from ARDS patients within 48 h of diagnosis of ARDS due to Gram-negative bacterial pneumonia. The following exclusion criteria were used: under 18 years old, pregnant, septic, aspiration and other non-bacterial forms of ARDS. In addition, 20 healthy volunteers served as the control group, and their BALF were all obtained via bronchoscopy. Approval of the medical ethics committees was obtained and all patients' relatives and volunteers provided written informed consent ( IRB{S} NO.2017121025 ) .

#### 2.1.2. BALF collection

The collection method for AMs was adapted from a previously described method [21]. Within 48 h of the patient being diagnosed with ARDS, the BALF was collected with a bronchial endoscope; the total amount used for lavage was 50 ml, and the total amount of recovered liquid was recorded to calculate the recovery rate. The BALF was filtered with gauze and centrifuged at 1200 rpm for 5 min at 4 °C, and the supernatant was stored at −80°. The cells were washed twice in RPMI 1640 containing 10% fetal bovine serum (FBS) and suspended in 10 ml of medium. The concentration of cell-free DNA (cf-DNA) bound to MPO (cf-DNA/MPO), a constituent of NET, was measured in BALF. Briefly, an antibody bound to the 96-well flat-bottom plate captured the enzyme MPO, and the amount of DNA bound to the enzyme was quantified using the Quant-iT™ PicoGreen kit (Invitrogen) [22]. The TNF-α, IL-6, IL-1β and IL-10 concentrations were also measured by ELISA, and the expression of M1 and M2 markers was detected by q-PCR (M1: iNOS; M2: CD206).

#### 2.1.3. In vivo experiments

**Mice.** C57BL/6 mice, male or female, aged 8–12 weeks, were purchased from the Experimental Animal Center of Central South University (Changsha, China). The mice were housed in microisolator cages under specific pathogen-free conditions. All animal experiments were approved by the Animal Care and Use Committee of Central South University (No.2017sydw00284).

**LPS/ALI Model.** Since our clinical specimens were collected from patients with ARDS caused by Gram-negative bacterial pneumonia, and one of the main pathogenic substances of Gram-negative bacteria is LPS, we used LPS intratracheal administration in the animal experiments to induce acute lung injury in mice and simulate human lung ARDS caused by Gram-negative pneumonia. We performed intratracheal injections as previously described [20,23]. After the administration of anesthesia, the trachea was exposed. A microsyringe was inserted into the trachea, and the mice received an intratracheal injection of LPS (*Escherichia coli* 0111: B4; Sigma-Aldrich, St. Louis, MO, USA) at a dose of 3 mg/kg in 60 μl of phosphate-buffered saline (PBS), followed by 200 μl of air to ensure deposition throughout each lung. The control mice received an intratracheal injection of 60 μl of PBS. Twenty-four hours later, the lungs were lavaged 3 times with 0.5 ml of PBS-EDTA (0.5 mM) for the determination of cell counts and differences in total protein. In separate experiments, the lungs were collected for immunohistochemistry and hematoxylin-eosin (HE) staining.

**Alveolar macrophage depletion.** Under anesthesia, the trachea was exposed via a midline neck incision and cannulated with a 30-gauge needle. The mice were then intratracheally administered 100 μl of clodronate liposomes (CLs) (YEASEN, Shanghai, China), which was diluted at a ratio of 1:1 in PBS. The control mice received the same volume of empty liposomes (PBS). Twenty-four hours later, adoptive transfer of polarized AMs into the lung was performed; the details are as follows.

**AM polarization.** AMs were isolated from mouse BALF and polarized to the M1 phenotype by LPS + IFN-γ stimulation or the M2 phenotype by IL-4 + IL-13 stimulation, as detailed in the in vitro experiment.

**Adoptive transfer of polarized AMs.** Thirty C57BL/6 mice, male or female, aged 8–12 weeks, were randomly divided into 6 groups: the control group, CL group, LPS-induced ALI group (LPS) group, AM-removed ALI group (LPS + CL), AM-removed ALI + M1-AM adoptive transfer group (LPS + CL + M1), and AM-removed ALI + M2-AM adoptive transfer group (LPS + CL + M2). Among these groups, the LPS + CL group, LPS + CL + M1 group and LPS + CL + M2 group were injected with CLs to remove mouse AMs. The control group and LPS group were given an equal dose of empty liposomes (PBS) instead of CLs. Twenty-four hours later, for the adoptive transfer group, M1 and M2 macrophages were transferred into the mouse lungs, half an hours later, LPS was injected into the mice via the trachea. Twenty-four hours later, the mice were sacrificed.

**NET inhibitor treatment.** In the treatment group, the mice were randomized into two groups that received instillations consisting of 200 μl of 3 mg/ml NE inhibitor (Alvelestat, Selleck, China) or 200 μl of 3 mg/ml PAD4 inhibitor (BB-Cl-Amidine, Cayman Chemical Company, Ann Arbor, Michigan, USA) by intraperitoneal injection. One hour later, LPS was injected into the mice via the trachea, as described above.

**Hematoxylin and eosin (HE) staining.** For histopathological analysis, the right lung lobes were fixed in 4% paraformaldehyde (PFA) and embedded in paraffin. Five-micron sections were placed onto glass slides and stained with HE. ALI severity was evaluated by assigning a semiquantitative histology score via a double-blind method, as described previously. Briefly, the histological index of lung damage included alveolar edema, hemorrhage, alveolar septal thickening and leukocyte infiltration [24]. Each item was divided into four grades

ranging from 0 to 3 (0 = normal; 1 = mild; 2 = moderate; and 3 = severe), and a total ALI score was then calculated.

**Quantification of BALF cf-DNA/MPO and protein levels.** cf-DNA/MPO in the BALF supernatant was quantified as described above. Protein concentrations in the BALF were quantified by performing a bicinchoninic acid protein assay (Biomiga, USA).

**Identification of NETs:** Paraffin-embedded mouse lungs were sectioned (4 μm), and the sections were prepared and mounted on glass slides. After the paraffin sections were dewaxed and dehydrated by gradient alcohol, antigen retrieval was performed using citrate buffer. The samples were permeabilized with 0.1% Triton X-100 for 10 min, following by blocking with 3% bovine serum albumin (BSA). The sections were incubated with primary antibodies, specifically, *anti*-citrullinated-histone H3 (Cit-H3, rabbit, 1:100; Abcam) and *anti*-myeloperoxidase (MPO, goat, 1:100; R&D Systems), followed by detection with FITC-conjugated donkey anti-rabbit IgG (H + L) (1:400; Servicebio, Wuhan, Hubei, China) and Cy3-conjugated donkey anti-goat IgG (H + L) (1:400; Servicebio) secondary antibodies, respectively, at room temperature for 1 h. DAPI was applied to detect DNA. The slides were visualized with an Olympus FluoView 500 confocal microscope.

**Flow cytometry.** Murine lungs were lavaged 8 times with 0.8 ml of 10 nM EDTA in PBS. BAL cells were filtered with a 40 μm filter and then collected by centrifugation. For immunostaining, the BAL was washed with 0.5% FBS and 5 nM EDTA in PBS, and cells were counted using a hemocytometer. The pellet was then incubated for 30 min at 4 °C in the dark in 100 μL of fluorescence-activated cell sorting (FACS) buffer with the following primary monoclonal antibodies for myeloid immunophenotype analysis: APC/CY7-labeled CD45, APC-labeled SiglecF, FITC-labeled CD11C, PE-labeled Ly6G, FITC-labeled CD11b, PerCP/Cy5.5-labeled CD54 and PE/CY7-labeled CD206 (Biolegend, San Diego, CA, USA). After centrifugation (350 rcf at 4 °C for 5 min), the pellet was resuspended in 500 μL of FACS buffer and analyzed on a BD flow cytometer. AMs were marked by CD45 + SiglecF + CD11C+; CD54 and CD11C were M1 AM markers, and CD206 was an M2 AM marker. Neutrophils were identified by the marker LY6G + CD11b+. CD45 is a marker of leukocytes. Because mouse alveolar macrophages express CD11C and SiglecF, CD11C positive expression indicated both M1 and M2, with the only difference between them being the intensity of the expression; therefore, we choose CD11C as the pan-marker of AM [25,26]. Each flow cytometric analysis was run on at least 100,000 cells, and the data were analyzed using FlowJo X.

**Immunohistochemistry.** The lungs of the mice were fixed with 4% PFA and embedded in paraffin. Histo-clear was used to deparaffinize the slices, and the slices were then rehydrated by an ethanol gradient. Bond HIER 2 (Leica Microsystems, Buffalo Grove, IL) was used for antigen retrieval at 100 °C for 20 min. The sections were incubated with *anti*-iNOS antibody (1:100, rabbit, Abcam) for 30 min at 21 °C, and proteins were detected by the Leica Bond Polymer DAB Refine, Peroxide Block and Mixed Refine DAB system. Reinfection was detected using Harris hematoxylin (Leica Microsystems).

### 2.1.4. In vitro experiments

**Isolation and purification of mouse bone marrow (BM) neutrophils.** BM cells were harvested from the femurs and tibias of 6- to 10-week-old C57BL/6 mice (SJA Laboratory Animal Co., Ltd, Changsha, Hunan, China). Neutrophils were separated from mononuclear cells by Ficoll centrifugation (d = 1.084 g/L) (GE, USA). Contaminating erythrocytes were removed by hypotonic lysis, and neutrophils were resuspended in PBS (Gibco Life Technologies, Grand Island, NY, USA) supplemented with 5% FBS (Wisent Biomart, Nanjing, Jiangsu, China).

**NET production, isolation and quantification.** BM neutrophils were seeded in duplicate wells of a 6-cm flat tissue culture dish. The cells were treated with PBS plus PMA (100 nM) for 4 h at 37 °C with 5% $CO_2$. After 4 h of stimulation, the supernatant and NET layer were aspirated, and the cells were removed by centrifugation at 200*g* for 5 min. Then, the supernatant was divided into 1.5-ml microcentrifuge tubes and centrifuged for 10 min at 12,000 g at 4 °C. The supernatant was discarded, and all obtained pellets were resuspended together in ice-cold PBS to a concentration corresponding to $2 \times 10^7$ neutrophils per 1000 μl of PBS. The DNA concentration in the obtained sample was measured as described above. The NETs were stored at −20 °C or −80 °C for subsequent experiments.

**Generation and activation of BM-derived macrophages (BMDMs).** BM cells were harvested from the femurs and tibias of 6- to 10-week-old C57BL/6 mice (SJA Laboratory Animal Co., Ltd). The cells were cultured in Dulbecco's modified Eagle's medium (DMEM) (Gibco) supplemented with 10% FBS (Wisent Biomart) and recombinant mouse M-CSF (40 ng/ml; PeproTech, Rocky Hill, NJ, USA). After 1 week, BMDMs were replated, and untreated (M0) macrophages were then stimulated with *Escherichia coli* LPS O111:B4 (100 ng/ml; Sigma) and IFN-γ (20 ng/ml; PeproTech) for 24 h (M1) or with IL-4 (20 ng/ml; PeproTech) for 24 h (M2). In addition, we used 2000 ng/ml NETs with or without 2 h of LPS pre-stimulation to stimulate M0 and M2 separately, and the cells were stimulated with LPS for 2 h as a comparison. The same grouping method was used for AMs.

**Isolation of AMs.** Alveolar lavage was performed as described above. BAL cells were collected by centrifugation. After red blood cell lysis, BAL cells were resuspended in DMEM containing 10% FBS and seeded in 24-well plates with cover glass at a density of $5 \times 10^4$ cells/well for 1 h. The cells were then thoroughly washed with PBS to remove all unattached cells, and attached macrophages were stimulated with the same method described for BMDMs.

**Immunofluorescence.** After fixation with 4% PFA for 20 min and permeabilization with 0.1% Triton X-100 for 2 min, the specimens were blocked with PBS containing 5% goat serum. The cells were incubated with primary antibodies, specifically *anti*-iNOS (1:50; mouse, Santa Cruz) and anti-CD206 (1:100; rabbit, Proteintech, Wuhan, Hubei, China) antibodies. The next steps were the same as those for the tissue immunofluorescence.

**Quantitative RT-PCR.** Total RNA from BMDMs was isolated with the RNeasy Micro Mini kit (Qiagen, Valencia, CA, Germany) and processed as previously described [27]. cDNA was synthesized from the RNA using the PrimeScript™ RT reagent kit with gDNA Eraser (Takara Biotechnology Co. Ltd., Dalian, China). Real-time qPCR was performed using SYBR® Premix Ex Taq™ II (Tli RNaseH Plus) (Takara Biotechnology Co. Ltd., Dalian, China) on an iCycler (ABI ViiATM7; Applied Biosystems, Carlsbad, CA, USA). The thermocycler parameters were set by the ABI 7500 Fast Real-time PCR system (Applied Biosystems)-associated SDS software version 2.3 (Applied Biosystems). Data were quantitated with the $2^{-\triangle\triangle Ct}$ method.

For each gene, an amplification curve was generated to evaluate the amplification efficiency. The sequences of the forward and reverse primers were as follows: human iNOS: forward 5′-TTCAGTATCACAAC CTCAGCAAG -3′ and reverse 5′-TGGACCTGCAAGTTAAAATCCC-3'; human CD206: forward 5′-GGGTTGCTATCACTCTCTATGC-3′ and reverse 5′-TTTCTTGTCTGTTGCCGTAGTT-3'; human GAPDH: forward 5′-CAAATGGGATGAAGCACTGA-3′ and reverse 5′-CGTCAAAGGTGGA GGAGTG-3'; mouse iNOS: forward 5′- GTTCTCAGCCCAACAATACA AGA-3′ and reverse 5′- GTGGACGGGTCGATGTCAC-3'; mouse Arg1: forward 5′- CTCCAAGCCAAAGTCCTTAGAG-3′ and reverse 5′- AGGAG CTGTCATTAGGGACATC-3'; and mouse GAPDH: forward 5′- AGGTCG GTGTGAACGGATTTG-3′ and reverse 5′- TGTAGACCATGTAGTTGAGG TCA-3'.

**Detection of macrophage surface markers by flow cytometry.** BMDMs were seeded in 6-well plates at a density of $8 \times 10^5$ cells/well. Cells treated with drugs or blank diluent were rinsed with warm PBS (37 °C). The cell suspensions were washed twice with ice-cold PBS before further processing. Flow cytometric analysis was performed as follows. The pellet was incubated for 20 min in 100 μL of FACS buffer with the following primary monoclonal antibodies for immunophenotype analysis. The cells were surface stained with F4/80

(Biolegend), CD11b, CD80, and CD86 (Biolegend), all diluted in PBS without Ca/Mg supplemented with 2% FCS and 2 mM EDTA [28]. The cells were fixed and permeabilized using the Cytofix/Cytoperm solution kit (Biolegend) according to the manufacturer's instructions and then subjected to intracellular staining for CD206 (Biolegend). F4/80 and CD11b are pan-BMDM markers, CD80 and CD86 are M1-like macrophage markers, and CD206 is a M2-like macrophage marker.

**ELISA.** ELISA cytokine assays (NeoBioscience, Shenzhen, Guangdong, China) were performed on the culture medium collected from murine macrophage cell cultures. The results are shown as concentrations derived from a standard curve. TNF-α, IL-1β, IL-6 and IL-10 were analyzed according to the manufacturer's instructions. TNF-α, IL-1β, and IL-6 are M1-like macrophage markers, IL-10 is M2-like macrophage marker.

**Western blot.** Western blot assays were performed using whole cell lysates. The membranes were then incubated with antibodies specific for CD206 (1:1000, Proteintech), Arg1 (1:1000, Servicebio), iNOS (1:1000, Abcam), or β-tubulin (1:2000, Servicebio) as an internal control.

**Statistical analyses.** The data are presented as the mean ± SD. Differences between two groups were assessed using a two-tailed Student's t-test, and differences among three or more groups were assessed with one-way ANOVA with Tukey's post hoc test. The tests were performed by GraphPad Prime 6 software (GraphPad, San Diego, CA, USA). Differences between groups were considered statistically significant when a confidence level of at least 95% ($P < 0.05$) was obtained.

## 3. Results

### 3.1. NET levels in ARDS patients positively correlate with M1-like macrophage polarization levels

BALF from healthy volunteers (control group) and patients with ARDS (within 48 h) who were diagnosed in the central ICU and respiratory ICU of Xiangya Hospital were collected. The baseline demographic parameters of the patients and the healthy control group are shown in Table 1(See S5 for details). cf-DNA/MPO and IL-6, TNF-α, IL-1β and IL-10 levels in BALF supernatants were detected. The mRNA levels of iNOS, CD206 were also detected. According to Fig. 1A, the cf-DNA/MPO level in BALF from ARDS patients (n = 20) was significantly higher than that in BALF from control group (n = 20), and the difference was statistically significant ($P < 0.01$). Fig. 1B shows that the levels of iNOS (Fig. 1B) mRNA in ARDS patients were significantly increased compared with those in the control group ($P < 0.01$), and although CD206 levels were decreased in ARDS patients, these results were not significant (Fig. 1C, $P = 0.0518$). Pearson correlation analysis was used to analyze the correlations between cf-DNA/MPO content and iNOS and CD206 mRNA levels in ARDS patients. iNOS mRNA levels were positively correlated with cf-DNA/MPO levels (Fig. 1D, $R = 0.8299$, $P < 0.01$). In addition, the levels of IL-6, TNF-α, and IL-1β cytokines in BALF supernatants from ARDS patients were significantly higher than those in BALF supernatants from the control group (Fig. 1F–H), and this difference was statistically significant ($P < 0.01$). There was an increase in IL-10 levels in several ARDS patients, but overall there was no difference between ARDS patients and the control group (Fig. 1I). Fig. 1J-L shows that IL-6, TNF-α, and IL-1β cytokine levels were positively correlated with cf-DNA/MPO levels in ARDS patients ($R = 0.8448$, 0.7767, and 0.8923, respectively). However, IL-10 levels (Fig. 1M) were not associated with cf-DNA/MPO levels in ARDS patients ($P = 0.5948$). IL-6, TNF-α, IL-1β and iNOS are M1 markers, and IL-10 and CD206 are M2 markers. Although we cannot determine whether M2 macrophages are reduced or not, we can speculate that M1 macrophages ratio maybe increased during the acute inflammatory phase of ARDS, and its polarization levels correlate positively with NET levels.

### 3.2. NET inhibitors attenuate LPS-induced ALI

Due to the increased cf-DNA/MPO production observed in BALF from ARDS patients, we further validated this phenomenon in animal experiments. An ALI animal model was established with LPS, and NET inhibitors (an NE inhibitor (Alvelestat), and a PAD4 inhibitor (BB-Cl-Amidine)) were administered at the same time. The cf-DNA/MPO level in the BALF was determined by the PicoGreen method. As expected, the cf-DNA/MPO level of the LPS-ALI group was the highest of all tested groups (Fig. 2A), while the cf-DNA/MPO levels of the NET inhibitor groups were significantly lower than that of the LPS group, and the difference was statistically significant ($P < 0.05$). To further verify that neutrophils recruited to the lungs during ALI can produce NETs, we also performed lung tissue immunofluorescence (Fig. 2B). Cit-H3 and MPO are the main components of NETs; therefore, Cit-H3 and MPO were selected as NET markers. Fig. 2B shows that there was no Cit-H3 or MPO polymer formation in the control group, while Cit-H3 and MPO polymers were most abundant in the LPS group; however, in the NET inhibitor groups (NE inhibitor, and PAD4 inhibitor), levels of Cit-H3 and MPO polymers were reduced compared to those in the LPS group. We conclude that NETs are produced in the ALI animal model and that NET inhibitors (an NE inhibitor and PAD4 inhibitor) can inhibit NET formation. The above results also confirmed the increased NET level observed in the clinical experiments.

Next, we evaluated the impact of NET formation on LPS-ALI. The mice were divided into the control group, LPS group, LPS + NE inhibitor group, and LPS + PAD4 inhibitor group. Pulmonary edema, alveolar congestion, alveolar septal thickening and leukocyte infiltration were most severe in the LPS group (Fig. 2C), and the lung injury score (Fig. 2D), number of neutrophils (Fig. 2E), total protein concentration in BALF (Fig. 2F) and pulmonary wet/dry (W/D) weights (Fig. 2G) were significantly reduced in the NE inhibitor and PAD4 inhibitor groups compared with those in the LPS group ($P < 0.001$). These results suggest that the inhibition of tissue damage by an NE inhibitor and PAD4 inhibitor may not only achieved by decreasing NETs generation, but also by reducing the infiltration of neutrophils, or both.

### 3.3. NET inhibitors mitigate M1-like macrophage polarization levels in LPS-induced ALI

Based on clinical data and the results of the above animal experiments, we concluded that NETs and macrophage polarization play important roles in the pathogenesis of ALI/ARDS, and NETs are positively correlated with M1 AM polarization. Therefore, we decided to explore the relationship between NETs and AM polarization in animal experiments. The animals were grouped as described above. Fig. 3A shows the results of immunohistochemical staining for iNOS in the lung tissue. The immunohistochemistry results demonstrate that the number of iNOS positive cells was highest in the LPS group and lower in the NET inhibitor groups than in the LPS group. Fig. 3B–J shows the flow cytometry results for AM polarization detection. CD45 + SiglecF + CD11C + are pan-AM markers. CD54 and CD11C are M1 markers, and CD206 is a M2 marker. After the AMs were labeled with CD45 + SiglecF + CD11C+, the expression of markers of polarized macrophages was compared. Fig. 3B–D shows that the alveolar macrophages in the LPS group accounted for the lowest proportion in the lavage fluid, while the proportion in the NET inhibitor groups increased (generally, the proportion of macrophages was greater than 90% in the control group; see S2 for details.), especially in the NE inhibitor group. This also indirectly reflects the possible inhibitory effect of inflammatory cell infiltration by NET inhibitors. S3 shows the proportion of neutrophils in the BALF of the different groups; the proportion of neutrophils in the LPS group was greater than 90%, whereas it was reduced in the NET inhibitor groups. Moreover, the proportion of neutrophils in the NE inhibitor group was slightly lower than that of the

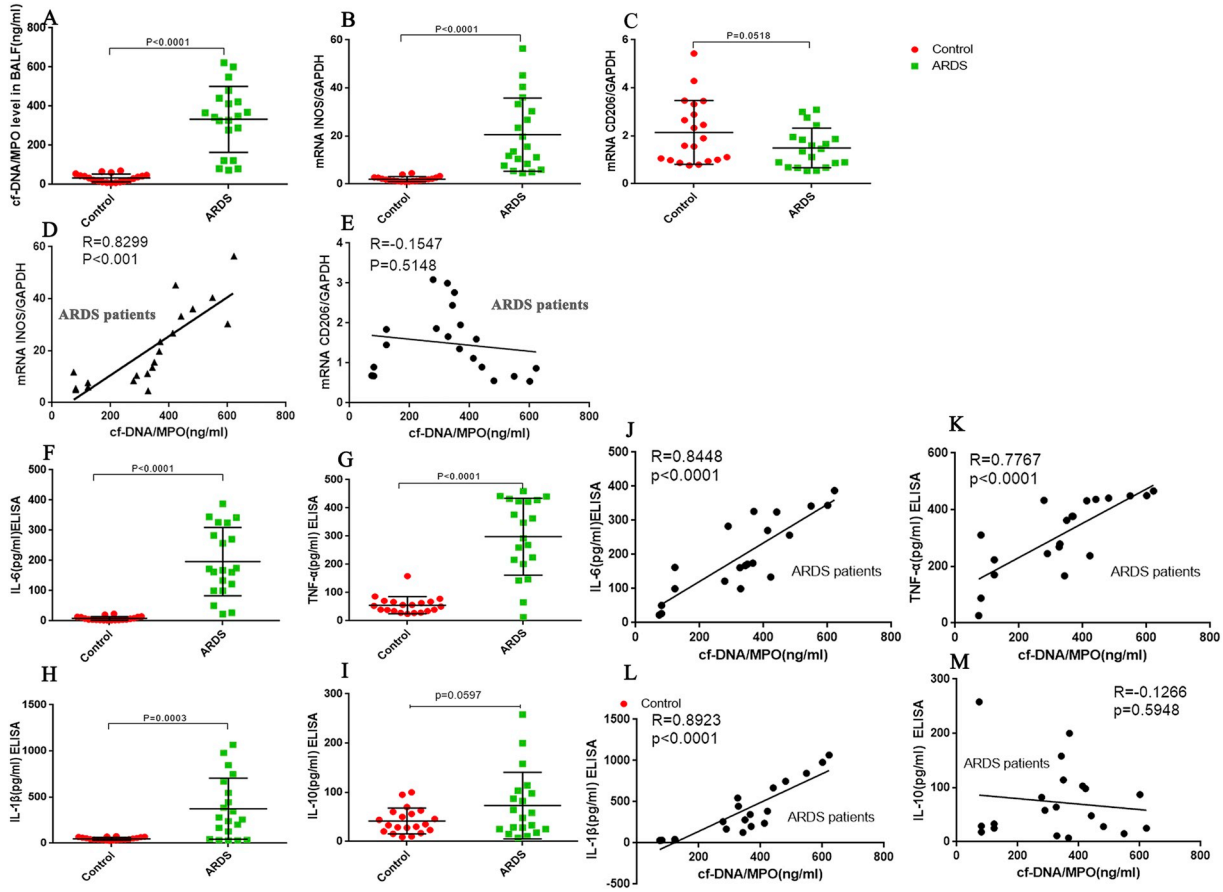


**Fig. 1.** NET levels in ARDS patients correlate positively with M1-like macrophage polarization levels. (A) The cf-DNA/MPO level in BALF from ARDS patients (n = 20) was significantly higher than that in BALF from the control group (n = 20), and this difference was statistically significant (P < 0.01). (B, C) Real-time qPCR showed that the mRNA levels of iNOS (B) in ARDS patients was significantly increased compared with those in the control group (P < 0.01), but there were no significant differences in CD206 (C) levels (P = 0.0518). (D–E) Pearson correlation analysis. The iNOS mRNA levels correlated positively with the cf-DNA/MPO levels (R = 0.8299, P < 0.01). (F-I) ELISA. The IL-6, TNF-α, and IL-1β cytokine levels in BALF supernatants from ARDS patients were significantly higher than those in BALF supernatants from the control group, and these differences were statistically significant (P < 0.01). There was an increase in IL-10 levels in several ARDS patients, but overall there was no difference between the ARDS and control group (Fig. 1I). (J–M) Pearson correlation analysis. The IL-6, TNF-α, and IL-1β cytokine levels correlated positively with the cf-DNA/MPO levels in ARDS patients (R = 0.8448, 0.7767, and 0.8923, respectively, P < 0.01); however, IL-10 levels (Fig. 1M) were not associated with cf-DNA/MPO levels (P = 0.5948) (n = 20).

PAD4 inhibitor group (See S3 for details). Besides, in the preliminary experiment of LPS groups, we found that when the lung inflammation is lighter, the proportion of macrophages is higher, and at the same time the proportion of neutrophils is lower. We did not show this part of the results in the article and in the supplementary data. These above results indicate that the NE inhibitor may have a greater inhibitory effect on neutrophil infiltration than the PAD4 inhibitor. This is probably because neutrophils and macrophages account for more than 90% of total BALF cells in ARDS; therefore, the proportion of alveolar macrophages in the NE inhibitor group is higher (Fig. 3C). The gray image indicates the control group. Fig. 3E, F, 3H, and 3I show that CD54 and CD11C had the strongest right shift in the LPS group, while CD54 and CD11C levels in the NET inhibitor group were lower than those in the LPS group but higher than those in the control group. However, the expression levels of CD206 showed the opposite pattern (Fig. 3G and J). The LPS group and the NET inhibitor groups were shifted to the left compared to the control group, which indicated that the expression of CD206 decreased. In addition, the expression level was lowest in the LPS group, while the degree of left shift was reduced when NET inhibitors were administered. These results indicate that NET inhibition can inhibit the polarization of AMs to the M1 type. According to Figs. 2B, Fig. 3B–D and S3, we hypothesize that the effect of NETs inhibitors on macrophage polarization may be due to two reasons: one is to affect the total number of cells that can produce NETs by affecting the infiltration of neutrophils, and the other may be some important components (Neutrophil elastase and Cit-H3) of NETs being inhibited, so that neutrophils cannot generate NETs. In a word, NETs may play an important role in the acute inflammatory response of ALI/ARDS. We also confirmed the proinflammatory role of M1 and the anti-inflammatory role of M2 AMs in LPS induced-ALI, and the detailed results are showed in S1.

### 3.4. NETs promote M1-like macrophage polarization

In the above clinical experiments and animal experiments, we learned that the polarization of M1 AMs and the formation of NETs play important roles in the inflammatory response during ARDS/ALI. Moreover, NETs correlate positively with M1-like macrophage polarization. In animal experiments, we observed that NET inhibitors have an inhibitory effect on M1 macrophage polarization. Therefore, mouse BM neutrophils were stimulated with PMA to generate NETs, which was quantified by PicoGreen. The mouse AMs were divided into 6 groups: the M0 group, M1 group (AMs were polarized with LPS and IFN-γ simultaneously for 24 h), M2 group (AMs were polarized with IL-4 for 24 h), NETs group (AMs were stimulated with NETs for 24 h), LPS group (AMs were stimulated with LPS for 2 h, and then LPS was removed and the AMs were further cultured for 24 h), LPS + NETs group (AMs were pre-stimulated with LPS for 2 h, and then the LPS was

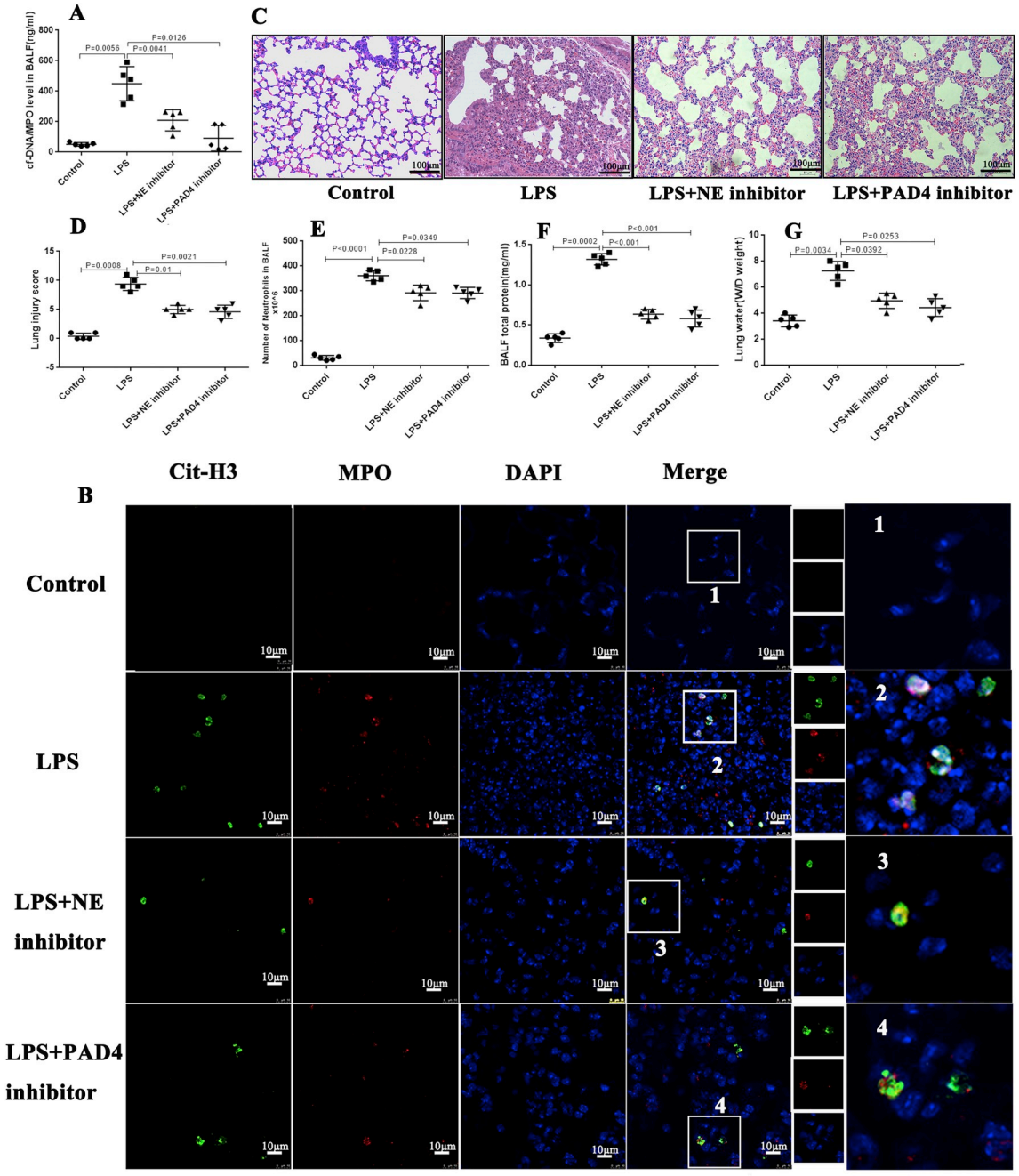


**Fig. 2.** NET inhibitors attenuate LPS-induced ALI in mice. (A) The PicoGreen method showed that the cf-DNA/MPO level of the LPS-ALI group was the highest of all the tested groups, while the cf-DNA/MPO levels of the NET inhibitor groups were significantly lower than that of the LPS group, and this difference was statistically significant ($P < 0.05$). (B) Lung tissue immunofluorescence showed that there was no Cit-H3 or MPO polymer formation in the control group, while Cit-H3 and MPO polymers were most abundant in the LPS group; however, in the NET inhibitor groups (NE inhibitor and PAD4 inhibitor), the levels of Cit-H3 and MPO polymers were reduced compared to those in the LPS group. (C) HE staining of lung sections (200 ×). (D) Lung injury scores. (E) The number of alveolar neutrophils in the BALF. (F) Total protein concentration in the BALF. (G) Lung water content. n = 5 mice/group. The results are representative of five separate independent experiments.

removed and NETs were added for continued stimulation for 24 h). Mouse BM-derived monocytes were also extracted and stimulated with M-CSF for 7 days to obtain mature M0 macrophages. The BMDMs were divided into 9 groups: the M0 group, M1 group (BMDMs were polarized with LPS and IFN-γ simultaneously for 24 h), M2 group (BMDMs were polarized with IL-4 for 24 h), NETs group (BMDMs were stimulated with NETs for 24 h), LPS group (BMDMs were stimulated with LPS for 2 h, and then LPS was removed and the BMDMs were further cultured for 24 h), LPS + NETs group (BMDMs were pre-stimulated with LPS for 2 h, and then the LPS was removed and NETs were added for continued stimulation for 24 h), M2 (IL-4)-NETs group (M2 macrophages were stimulated with NETs for 24 h), M2 (IL-4)-LPS group (M2 macrophages were stimulated with LPS for 2 h, then removed LPS and continued culturing for 24 h), and M2 (IL-4)-LPS + NETs group (M2 macrophages were pre-stimulated with LPS for 2 h, and then the LPS was removed and NETs were added for continued stimulation for 24 h). Fig. 4A shows the confocal microscopy results for AMs. iNOS and CD206 are markers of M1 and M2 macrophages, respectively. The figure shows that in AMs, the expression of iNOS increased after stimulation with NETs or LPS, and when LPS and NETs were combined, the increase in iNOS levels was most pronounced. Fig. 4B shows the Western blot results for BMDMs; CD206 and Arg1 are markers of M2 macrophages. The Western

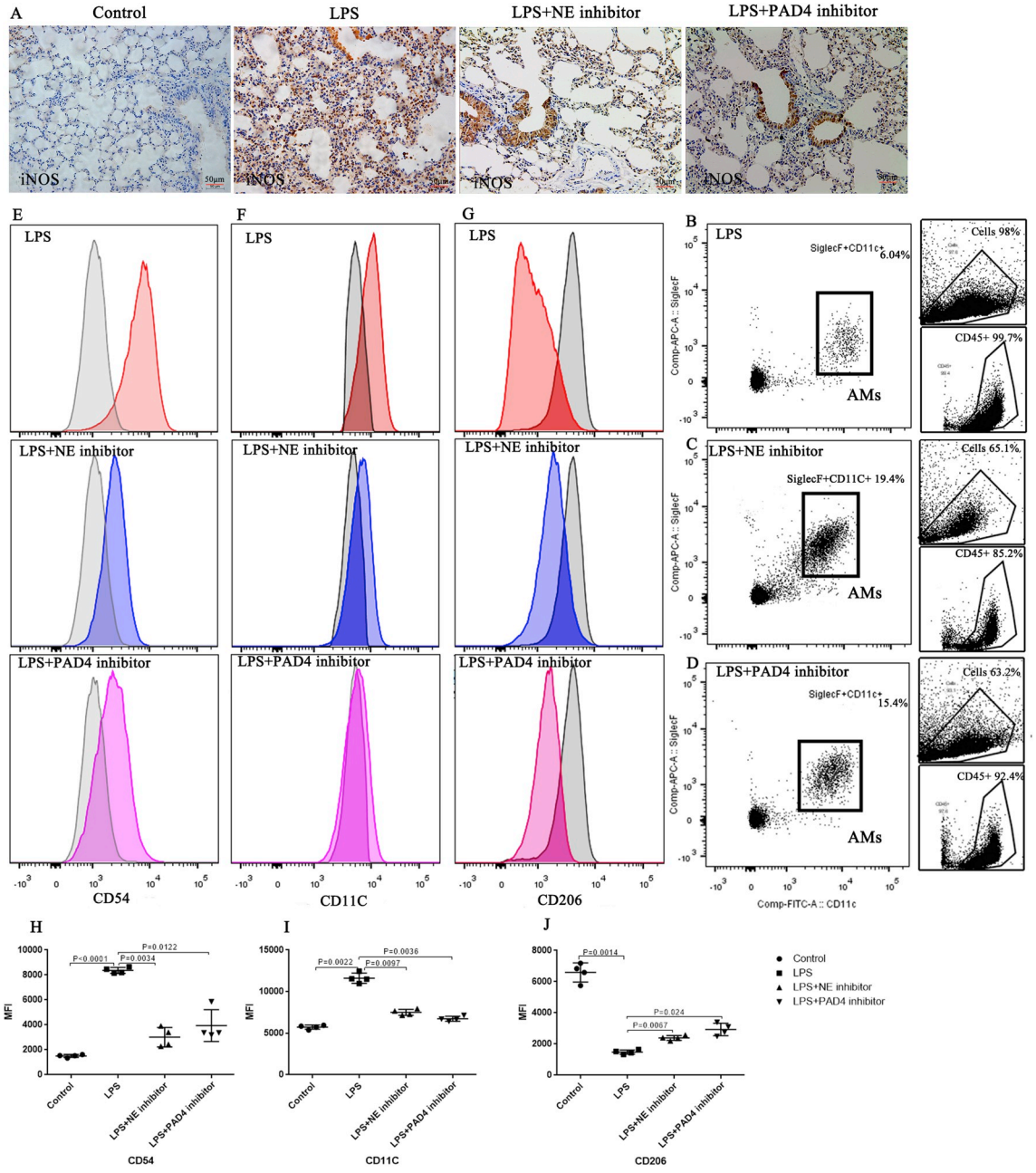


**Fig. 3.** NET inhibitors mitigate M1-like macrophage polarization levels in LPS-induced ALI. (A) Immunohistochemistry of iNOS in lung tissue. The number of iNOS positive cells was highest in the LPS group but lower in the NET inhibitor groups than in the LPS group. (B–G) Flow cytometry. CD45 + SiglecF + CD11C + were pan-AM markers, CD54 and CD11C are M1 markers, and CD206 is a M2 marker. The gray image indicates the control group. CD54 and CD11C had the strongest right shift in the LPS group, while CD54 and CD11C levels in the NET inhibitor group were lower than those in the LPS group but higher than those in the control group. However, the expression levels of CD206 showed the opposite pattern. (H–J) To identify changes in the expression of CD54, CD11C and CD206, we calculated the mean fluorescence intensity (MFI) of CD54, CD11C and CD206 (n = 4).

blot results show that the protein levels of CD206 and Arg1 were highest in M2 macrophages, while the expression of CD206 and Arg1 decreased after M2 macrophages were stimulated with NETs (M2-NETs) and LPS (M2-LPS), and the expression of CD206 and Arg1 decreased most in the M2-LPS + NETs group. The difference of CD206 between the M2-LPS + NETs and M2 groups was statistically significant (P = 0.0067), as well as Arg1(P = 0.0204). After stimulation with LPS, NETs and LPS + NETs, the CD206 expression and Arg1 expression of M2 macrophages were significantly lower than those of unstimulated M2 macrophages, and the greatest decrease was observed in the M2-LPS + NETs group. However, the expression level of iNOS showed the opposite pattern. The expression of iNOS in M1 macrophages was significantly increased. In M2 macrophages, the expression of iNOS in the M2-LPS + NETs group was higher than that in the M2 control group. This difference was statistically significant (P = 0.0065).

We also conducted flow cytometry to further verify the above results. Fig. 5A shows the results of BMDM flow cytometry. F4/80 + CD11b + are pan-BMDM markers, CD206 is a marker of M2 macrophages, and CD80 and CD86 are markers of M1 macrophages. The gray pattern shows the expression of the M0 macrophage marker. To identify the expression of CD206, CD80 and CD86, we calculated the MFI of CD206, CD80 and CD86 (Fig. 5B–D). The expression of CD80 and CD86 in the M1 (LPS + IFN-γ) group was significantly higher than that in the M0 group, and the expression of CD206 was slightly

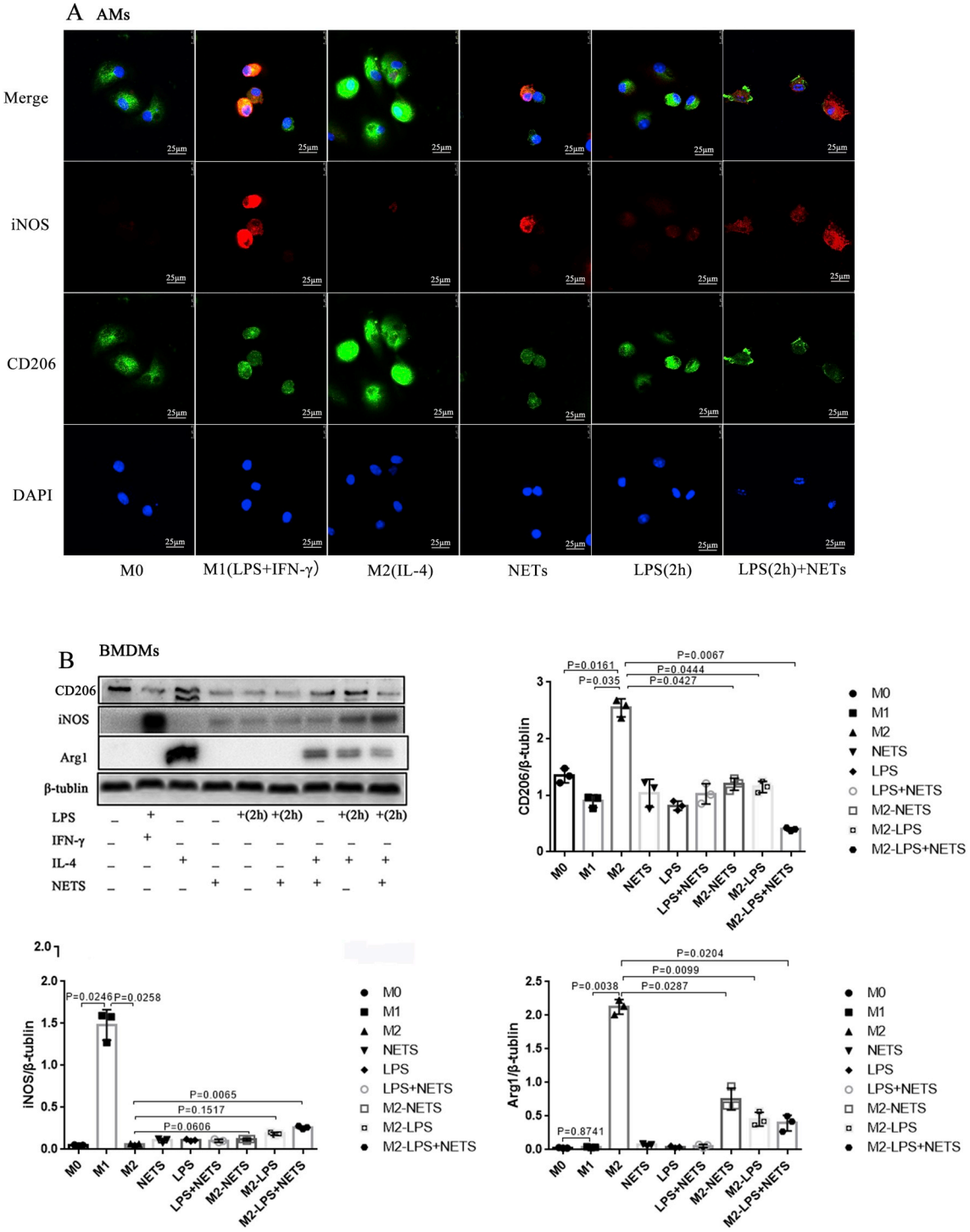


**Fig. 4.** NETs promote M1-type macrophage polarization. (A) Confocal results for AMs. iNOS and CD206 are markers of M1 and M2 macrophages, respectively. In AMs, the expression of iNOS increased after stimulation with NETs or LPS, and when LPS and NETs were combined, the increase in iNOS levels was the most pronounced. (B) Western blot results for BMDMs. CD206 and Arg1 are markers of M2 macrophages. The Western blot results showed that the protein levels of CD206 and Arg1 were the highest in M2 macrophages, while the expression of CD206 and Arg1 decreased after stimulation with NETs (M2-NETs) and LPS (M2-LPS), the expression of CD206 and Arg1 decreased the most in the M2-LPS + NETs group. These differences were statistically significant ($P < 0.05$). n = 3.

decreased; in contrast, CD206 in the M2 (IL-4) group was significantly increased, and the expression of CD80 and CD86 was slightly reduced. After stimulating M0 and M2 macrophages with NETs in the presence or absence of LPS, the expression levels of CD80 and CD86 were all significantly increased compared with those in the M0 and M2 groups, and CD206 expression was slightly decreased in M0 macrophages (LPS, NETs, and LPS + NETs); however, the decreased level of CD206 expression was more pronounced in M2 macrophages (M2-LPS, M2-NETs, M2-LPS + NETs). This phenomenon was most significant in the LPS + NETs and M2-LPS + NETs groups. Fig. 5E–H shows the ELISA and PCR results. TNF-α and IL-6 were mainly secreted by M1 macrophages. TNF-α and IL-6 levels in M1 macrophages were significantly higher than those in M0 and M2 macrophages. In terms of M0 macrophages, TNF-α and IL-6 levels were also increased most in the

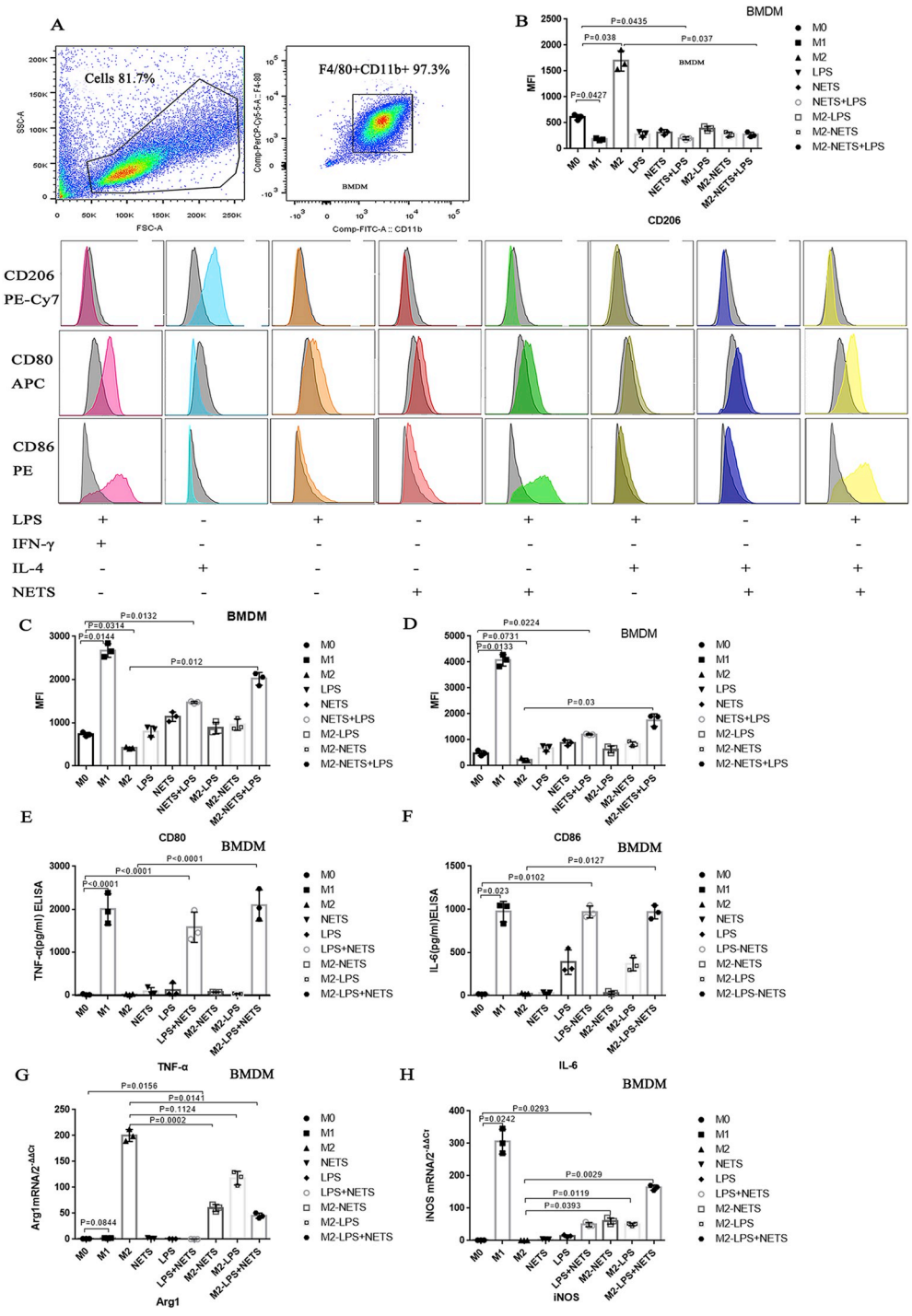


**Fig. 5.** NETs promote M1-type macrophage polarization. (A) Flow cytometry of BMDMs. F4/80 + CD11b + is a pan-BMDM marker, CD206 is a marker of M2 macrophages, and CD80 and CD86 are markers of M1 macrophages. (B–D) To identify the expression of CD206, CD80 and CD86, we calculated the MFI of CD206, CD80 and CD86. (E, F) We used M1 as a positive control, and the ELISA results showed that TNF-α and IL-6 levels in M1 macrophages were significantly higher than those in M0 and M2 macrophages. In the presence of LPS and NETs, TNF-α and IL-6 levels increased compared to those of M0 macrophages, and similar results were obtained when comparing M2-LPS + NETs to M2 macrophages ($P < 0.05$). (G, H) RNA results for Arg1 and iNOS. n = 3.

LPS + NETs group. The same result was observed when the M2-LPS + NETs group was compared to the other M2 macrophages groups. The Arg1 and iNOS results in Fig. 5G and H were consistent with the Western blot results. All above results indicate that NETs polarize macrophages to the M1 phenotype, and pre-stimulation with LPS has a synergistic effect.

## 4. Discussion

A growing number of studies have shown that the diversity of AMs is a key regulator of the development and recovery of ALI/ARDS, and different subtypes play different roles at different stages [29,30]. AMs are classified into two types, namely, classical activated macrophages (M1) and noncanonically activated macrophages (M2), according to their expression of surface markers, chemokines, secreted cytokines and transcription factors. M1 macrophages can secrete proinflammatory factors, such as TNF-α and IL-6, express iNOS and upregulate CD54 or CD11C markers. In contrast, M2 macrophages can downregulate proinflammatory factors and express Arg1, CD206, CD71 and other proteins [30].

There are many studies on macrophage subpopulations, and the markers of macrophages in different organs or tissues are different. Some subsets lack specific markers and need to be labeled with a combination of markers. For in vivo experiments, $CD45^{+}$ CD11C + Siglec F+ are currently preferred for labeling mouse AMs [30], mostly for flow cytometry. However, there is no good set of

markers for labeling human AMs for flow cytometry. Most studies have been limited to immunohistochemistry for subgrouping [3,31,32]. In general, simply dividing the AMs into M0, M1, and M2 subtypes by one or several markers is not rigorous. Macrophage plasticity causes dynamic changes, and macrophages can easily switch types. A variety of heterozygous phenotypes can occur based on changes in the microenvironment in the lungs [3,4,33]. In this case, simply using markers to divide different subgroups may be inaccurate. Thus, studies on the overall functional changes of AMs, such as changes in cytokine levels and changes in functional protein levels, may be more meaningful for analyzing changes in macrophage subtypes during different stages of the disease. Therefore, the in vivo experiments in this study did not investigate the changes in the proportions of AMs during the acute inflammation stage of ALI/ARDS but focused on overall phenotypic changes and functional changes from a macro perspective.

Our previous animal studies have shown that neutrophils can produce NETs during the acute inflammatory reaction of ARDS [20,34]. NETs are known to be a double-edged sword; appropriate NET production can enhance the ability of neutrophils to capture and kill pathogens, but excessive NET production often causes severe inflammatory reactions and tissue damage [35,36]. In ARDS, NETs tend to be excessive, so their destructive effect outweighs their bactericidal effect. Moreover, NETs are complex, and many associated factors, such as LL37 and MPO, can promote M1-like polarization of macrophages, further aggravating the inflammatory response [18].

According to our clinical findings, the mRNA levels of iNOS in AMs and the cytokine levels of TNF-α, IL-6, and IL-1β were higher in the acute inflammatory response period of ALI/ARDS than in the healthy control group; however, the mRNA levels of CD206 and the IL-10 level in BALF did not change significantly; this finding indirectly reflects the predominance of M1 AMs in the early stage of ARDS, which is consistent with previous studies [29,33]. In addition, we found that the level of cf-DNA/MPO (NETs level) in BALF was also significantly increased during the inflammatory response. A Pearson correlation study revealed that the NET levels in ARDS patients were positively correlated with IL-6 and TNF-α mRNA levels and with IL-6, TNF-α, and IL-1β cytokine levels in BALF. Interestingly, in some patients with ARDS, IL-10 levels were elevated, possibly as a result of a large release of pro-inflammatory factors that activate anti-inflammatory responses. However, this increase in IL-10 levels is less than the local production of inflammatory factors, and thus is unable to exert sufficient biological activity; therefore, the inflammatory mediators IL-6, TNF-α and IL-1β were still increased. We conclude that there may be a relationship between NETs and the polarization of M1-like AMs. According to relevant reports in the literature [18], we speculate that NETs may play a role in promoting macrophage M1-like polarization. In animal experiments, we observed that two types of NET inhibitors (the NE inhibitor Alvelestat, and the PAD4 inhibitor BB-Cl-Amidine) can reduce lung damage, alveolar edema, alveolar cavity protein deposition, neutrophil infiltration and the level of inflammatory factors. These results demonstrate that the inhibition of lung inflammation caused by NET inhibitors may be through NET inflammation inhibition as well as indirectly by decreasing the infiltration of neutrophils. In addition, we found that NET inhibitors (the NE inhibitor Alvelestat, and the PAD4 inhibitor BB-Cl-Amidine) can inhibit M1 macrophage polarization. Immunohistochemistry showed that the expression of iNOS was significantly increased in the LPS-ALI group but decreased in the inhibitor group. Flow cytometry also showed that the M1 markers CD54 and CD11C increased in the LPS-ALI group, and the elevated levels in the inhibitor groups were lower than those in the LPS group. However, the CD54 and CD11C levels in the inhibitor group were still higher than those in the control group, and the level of the M2 marker CD206 showed the opposite pattern. Interestingly, CD71, another marker of M2 macrophages, did not change significantly between the LPS group and the inhibitor group (not shown in this article; the details are shown in S4). Thus, we cannot judge the polarization state of macrophages based on a single marker change.

By removing AMs from ALI mice and adoptively transferring M1 AMs and M2 AMs, we found that the M1 AM adoptive transfer group had increased lung histopathological damage compared to that in the AM-removed LPS group (the details are shown in S1). These results indicate that when lungs develop an inflammatory reaction, AMs can polarize to the M1 phenotype to participate in the proinflammatory response. Compared with the AM-removed group, the M2 AM adoptive transfer group showed a significantly reduced lung injury score, a marked reduction in lung edema (W/D), a marked decrease in protein content, and a decrease in inflammatory factor expression in BALF when LPS was used to stimulate the lungs. We conclude that M2 AMs mainly play a role in alleviating lung damage and promoting tissue repair during this process.

The above results demonstrate that AMs play an important regulatory role in the pathogenesis of LPS-induced ALI, in which M1 AMs are involved in aggravating the degree of inflammatory infiltration into the lung tissue in ALI mice, whereas M2 AMs have the opposite effect. These findings were consistent with existing research [11,37]. In addition, NET inhibitors may attenuate lung tissue inflammation by inhibiting the conversion of AMs to the M1 phenotype.

To verify the phenomenon observed in the in vivo experiment, in vitro cell experiments were performed. In cell experiments, when high concentrations of NETs (2000 ng/ml) were used to stimulate mouse BMDMs (M0) and AMs (M0), especially after pre-stimulation with LPS for 2 h, the macrophages began to exhibit M1 characteristics. We can refer to such macrophages as M1-like macrophages. When M2 macrophages were exposed to NETs (2000 ng/ml), M2 macrophages were more sensitive than M0 macrophages, and the inflammatory indicators increased more than in the stimulated M0 macrophages. In addition, Arg1 and CD206 levels were significantly lower than those in the control group, especially after LPS pre-stimulation for 2 h, and the changes in Arg1 and CD206 protein levels were the greatest. We conclude that M2 macrophages are more susceptible to NETs than M0 macrophages in terms of the ability to polarize to inflammatory macrophages, indicating that when the ARDS inflammatory response cannot be effectively controlled, the M2 macrophages present during the repair phase are easily converted to M1 macrophages; as a result, the acute inflammatory response period is prolonged. These findings also show that during the recovery period, when the lungs are exposed to external stimuli, such as bacteria and wounds, a second time, it is easy to reproduce the inflammatory reaction; as a result, the tissue damage is aggravated.

In conclusion, during the acute inflammatory response period of ARDS, the M1 polarization level is increased, and the NET level is often excessive during ALI/ARDS, which can polarize macrophages to the M1 phenotype. At the cellular level, when LPS is used to pre-stimulate macrophages to mimic the in vivo environment, high concentrations of NETs can shift M0 and M2 macrophages toward M1 macrophages, which may aggravate ALI/ARDS lung tissue damage. The transformation to M1 macrophages aggravates the inflammatory response. M0 macrophages are reactive at rest, even if M1 polarization is reduced, but there is no increase in the M2 phenotype, which is also not conducive to the repair of damaged lung tissue. This study demonstrates that NETs can promote inflammatory responses by affecting the polarization of macrophages, especially in the presence of LPS; however, no specific pathways have been studied. We have completed RNA sequencing and will continue to conduct pathway screening studies in subsequent research to provide a more empirical basis for polarization regulation. The reason why the NE inhibitor Alvelestat has a greater inhibitory effect on neutrophil inflammatory infiltration than the PAD4 inhibitor BB-Cl-Amidine has not been studied in this experiment, and there is currently no relevant literature exploring these effects, which may be related to their different statuses in neutrophils. Thus, we will explore this issue further in future research.

## Authorship

Patients' BALF and clinical data collection were performed by Pengbo D, Jinjin L and Haitao L. Animal experiments were performed by Chao S, Yi L, Minhui D, Zhi M and Qian L. Flow cytometry was performed by Lemeng Zhang. HE staining was performed by Hongyi T. Western blot was performed by Yuan L. PCR, ELISA and Immunofluorescence were performed by Chao S, Fengyu L. Invitro experiments were performed by Chao S, Yanjun Z and Yifei F. The manuscript was drafted by Chao S, with critical revisions made by Pinhua P, Bailing L, Chengping Hu and Xiaoli Su. This study was conceived of and designed by Chao S, Shuai L and Pinhua P.

## Conflict-of-interest disclosure

The authors declare that they have no conflict of interests.

## Acknowledgments

Thanks to American Journal Experts for providing language retouching services. This work was supported by the National Natural Science Foundation of China(no. 81770080) and Ministry of Science and Technology of the People's Republic of China(no. 2016YFC1304204).

## Appendix A. Supplementary data

Supplementary data to this article can be found online at https://doi.org/10.1016/j.yexcr.2019.06.031.

## References

[1] Acute respiratory distress Syndrome：The Berlin definition, J. Am. Med. Assoc. 307 (23) (2012 Jun 20) 2526–2533.
[2] H. Dong, J. Li, Y. Lv, Y. Zhou, G. Wang, S. Hu, X. He, P. Yang, Z. Zhou, X. Xiang, C.Y. Wang, Comparative analysis of the alveolar macrophage proteome in ALI/ARDS patients between the exudative phase and recovery phase, BMC Immunol. 14 (2013) 25.
[3] N.R. Aggarwal, L.S. King, F.R. D' Alessio, Diverse macrophage populations mediate acute lung inflammation and resolution, Am. J. Physiol. Lung Cell Mol. Physiol. 306 (2014) L709–L725.
[4] E. Bazzan, C. Rigobello, D. Biondini, M. Schiavon, F. Lunardi, S. Baraldo, F. Rea, P. Simioni, F. Calabrese, M. Saetta, M.G. Cosio, Dual polarization of human alveolar macrophages progressively increases with smoking and COPD severity, Respir. Res. 18 (1) (2017) 40.
[5] G. Bellani, J.G. Laffey, T. Pham, E. Fan, L. Brochard, A. Esteban, L. Gattinoni, F. van Haren, A. Larsson, D.F. McAuley, M. Ranieri, G. Rubenfeld, B.T. Thompson, H. Wrigge, A.S. Slutsky, A. Pesenti, Epidemiology, patterns of care, and mortality for patients with acute respiratory distress syndrome in intensive care units in 50 countries, J. Am. Med. Assoc. 315 (8) (2016) 788–800.
[6] J. Cohen, The immunopathogenesis of sepsis, Nature 420 (2002) 885–891.
[7] J.G. Norman, G.W. Fink, M.G. Franz, Acute pancreatitis induces intrapancreatic tumor necrosis factor gene expression, Arch. Surg. 130 (9) (1995) 966–970.
[8] V. Papayannopoulos, K.D. Metzler, A. Hakkim, A. Zychlinsky, Neutrophil elastase and myeloperoxidase regulate the formation of neutrophil extracellular traps, J. Cell Biol. 191 (2010) 677–691, https://doi.org/10.1083/jcb.201006052.
[9] W.Y. Park, R.B. Goodman, K.P. Steinberg, J.T. Ruzinski, F. Radella 2nd, D.R. Park, J. Pugin, S.J. Skerrett, L.D. Hudson, T.R. Martin, Cytokine balance in the lungs of patients with acute respiratory distress syndrome, Am. J. Respir. Crit. Care Med. 164 (2001) 1896–1903.
[10] T.M. Siler, J.E. Swierkosz, T.M. Hyers, A.A. Fowler, R.O. Webster, Immunoreactive interleukin-1 in bronchoalveolar lavage fluid of high-risk patients and patients with the adult respiratory distress syndrome, Exp. Lung Res. 15 (1989) 881–894.
[11] B.T. Thompson, R.C. Chambers, K.D. Liu, Acute respiratory distress syndrome, N. Engl. J. Med. 377 (19) (2017) 1904–1905.
[12] F.R. D'Alessio, J.M. Craig, B.D. Singer, D.C. Files, J.R. Mock, B.T. Garibaldi, J. Fallica, A. Tripathi, P. Mandke, J.H. Gans, N. Limjunyawong, V.K. Sidhaye, N.M. Heller, W. Mitzner, L.S. King, N.R. Aggarwal, Enhanced resolution of experimental Ards through Il-4-mediated lung macrophage reprogramming, Am. J. Physiol. Lung Cell Mol. Physiol. 310 (2016) L733–L746.
[13] J. Van den Bossche, J. Baardman, N.A. Otto, S. van der Velden, A.E. Neele, S.M. van den Berg, R. Luque-Martin, H.J. Chen, M.C. Boshuizen, M. Ahmed, M.A. Hoeksema, A.F. de Vos, M.P. de Winther, Mitochondrial dysfunction prevents repolarization of inflammatory macrophages, Cell Rep. 17 (3) (2016) 684–696.
[14] V. Brinkmann, U. Reichard, C. Goosmann, B. Fauler, Y. Uhlemann, D.S. Weiss, Y. Weinrauch, A. Zychlinsky, Neutrophil extracellular traps kill bacteria, Science 303 (2004) 1532–1535, https://doi.org/10.1126/science.1092385.
[15] T. Saitoh, J. Komano, Y. Saitoh, T. Misawa, M. Takahama, T. Kozaki, T. Uehata, H. Iwasaki, H. Omori, S. Yamaoka, N. Yamamoto, S. Akira, Neutrophil extracellular traps mediate a host defense response to human immunodeficiency virus-1, Cell Host Microbe 12 (2012) 109–116, https://doi.org/10.1016/j.chom.2012.05.015.
[16] H. Huang, S. Tohme, A.B. Al-Khafaji, S. Tai, P. Loughran, L. Chen, S. Wang, J. Kim, T. Billiar, Y. Wang, A. Tsung, Damage-associated molecular pattern-activated neutrophil extracellular trap exacerbates sterile inflammatory liver injury[J], Hepatology 62 (2) (2015) 600–614.
[17] M. Merza, H. Hartman, M. Rahman, R. Hwaiz, E. Zhang, E. Renstrom, L. Luo, M. Morgelin, S. Regner, H. Thorlacius, Neutrophil extracellular traps induce trypsin activation, inflammation, and tissue damage in mice with severe acute pancreatitis, Gastroenterology 149 (7) (2015) 1920–1931.
[18] J.M. Kahlenberg, C. Carmona-Rivera, C.K. Smith, M.J. Kaplan, Neutrophil extracellular trap-associated protein activation of the NLRP3 inflammasome is enhanced in lupus macrophages, J. Immunol. 190 (3) (2013) 1217–1226.
[19] A. Lee, M.K. Whyte, C. Haslett, Inhibition of apoptosis and prolongation of neutrophil functional longevity by inflammatory mediators, J. Leukoc. Biol. 54 (1993) 283–288.
[20] S. Liu, X. Su, P. Pan, L. Zhang, Y. Hu, H. Tan, D. Wu, B. Liu, H. Li, Y. Li, M. Dai, Y. Li, C. Hu, A. Tsung, Neutrophil extracellular traps are indirectly triggered by lipopolysaccharide and contribute to acute lung injury, Sci. Rep. 6 (2016) 37252.
[21] A.B. Cohen, M.J. Cline, The human alveolar macrophage: isolation, cultivation in vitro, and studies of morphologic and functional characteristics, J. Clin. Investig. 50 (7) (1971) 1390–1398.
[22] P.G. Czaikoski, J.M. Mota, D.C. Nascimento, F. Sonego, F.V. Castanheira, P.H. Melo, G.T. Scortegagna, R.L. Silva, R. Barroso-Sousa, F.O. Souto, A. Pazin-Filho, F. Figueiredo, J.C. Alves-Filho, F.Q. Cunha, Neutrophil extracellular traps induce organ damage during experimental and clinical sepsis, PLoS One 11 (2) (2016) e0148142.
[23] L. Wang, L. Zhao, J. Lv, Q. Yin, X. Liang, Y. Chu, R. He, BLT1-dependent alveolar recruitment of CD4(+) CD25(+) Foxp3(+) regulatory T cells is important for resolution of acute lung injury, Am. J. Respir. Crit. Care Med. 186 (2012) 989–998.
[24] M. Dai, P. Pan, H. Li, S. Liu, L. Zhang, C. Song, Y. Li, Q. Li, Z. Mao, Y. Long, X. Su, C. Hu, The antimicrobial cathelicidin peptide hlF(1-11) attenuates alveolar macrophage pyroptosis induced by Acinetobacter baumannii in vivo, Exp. Cell Res. 364 (1) (2018) 95–103.
[25] A.J. Byrne, T.M. Maher, C.M. Lloyd, Pulmonary macrophages: a new therapeutic pathway in fibrosing lung disease? Trends Mol. Med. 22 (4) (2016) 303–316.
[26] E.M. Todd, J.Y. Zhou, T.P. Szasz, L.E. Deady, J.A. D'Angelo, M.D. Cheung, A.H. Kim, S.C. Morley, Alveolar macrophage development in mice requires L-plastin for cellular localization in alveoli, Blood 128 (24) (2016) 2785–2796.
[27] M.F. Nie, Q. Xie, Y.H. Wu, H. He, L.J. Zou, X.L. She, X.Q. Wu, Serum and ectopic endometrium from women with endometriosis modulate macrophage M1/M2 polarization via the smad2/smad3 pathway, J. Immunol. Res. 2018 (2018) 6285813.
[28] S. Rosseau, P. Hammerl, U. Maus, H.D. Walmrath, H. Schutte, F. Grimminger, W. Seeger, J. Lohmeyer, Phenotypic characterization of alveolar monocyte recruitment in acute respiratory distress syndrome, Am. J. Physiol. Lung Cell Mol. Physiol. 279 (1) (2000) L25–L35.
[29] X. Huang, H. Xiu, S. Zhang, G. Zhang, The role of macrophages in the pathogenesis of ALI/ARDS, Mediat. Inflamm. 2018 (2018) 1264913.
[30] L.K. Johnston, C.R. Rims, S.E. Gill, J.K. McGuire, A.M. Manicone, Pulmonary macrophage subpopulations in the induction and resolution of acute lung injury, Am. J. Respir. Cell Mol. Biol. 47 (4) (2012) 417–426.
[31] A.J. Byrne, T.M. Maher, C.M. Lloyd, Pulmonary macrophages: a new therapeutic pathway in fibrosing lung disease? Trends Mol. Med. 22 (4) (2016) 303–316.
[32] Y. Kaku, H. Imaoka, Y. Morimatsu, Y. Komohara, K. Ohnishi, H. Oda, S. Takenaka, M. Matsuoka, T. Kawayama, M. Takeya, T. Hoshino, Overexpression of CD163, CD204 and CD206 on alveolar macrophages in the lungs of patients with sever e chronic obstructive pulmonary disease, PLoS One 9 (1) (2014) e87400.
[33] G.W. Tu, Y. Shi, Y.J. Zheng, M.J. Ju, H.Y. He, G.G. Ma, G.W. Hao, Z. Luo, Glucocorticoid attenuates acute lung injury through induction of type 2 macrophage, J. Transl. Med. 15 (1) (2017) 181.
[34] H. Li, X. Zhou, H. Tan, Y. Hu, L. Zhang, S. Liu, M. Dai, Y. Li, Q. Li, Z. Mao, P. Pan, X. Su, C. Hu, Neutrophil extracellular traps contribute to the pathogenesis of acid-aspiration-induced ALI/ARDS, Oncotarget 9 (2) (2018) 1772–1784.
[35] B.G. Yipp, B. Petri, D. Salina, C.N. Jenne, B.N. Scott, L.D. Zbytnuik, K. Pittman, M. Asaduzzaman, K. Wu, H.C. Meijndert, S.E. Malawista, de Boisfleury, A. Chevance, K. Zhang, J. Conly, P. Kubes, Infection-induced NETosis is a dynamic process involving neutrophil multitasking in vivo, Nat. Med. 18 (9) (2012) 1386–1393.
[36] M. Toussaint, D.J. Jackson, D. Swieboda, A. Guedan, T.D. Tsourouktsoglou, Y.M. Ching, F. Farnir, V. Papayannopoulos, F. Bureau, T. Marichal, S.L. Johnston, Host DNA released by NETosis promotes rhinovirus-induced type-2 allergic asthma exacerbation, Nat. Med. 23 (6) (2017) 681–691.
[37] C.Y. Yang, C.S. Chen, G.T. Yiang, Y.L. Cheng, S.B. Yong, M.Y. Wu, C.J. Li, New insights into the immune molecular regulation of the pathogenesis of acute respiratory distress syndrome, Int. J. Mol. Sci. 19 (2) (2018).